Design optimization of PCM-based finned heat sinks for mechatronic components: A numerical investigation and parametric study

Bessem Debich, Abdelkhalak El Hami, Ahmed Yaich, Wajih Gafsi, Lassaad Walha, Mohamed Haddar

Design optimization of PCM-based finned heat sinks for mechatronic components: A numerical investigation and parametric study

Bessem DEBICH [1, 2], Abdelkhalak EL HAMI [1], Ahmed YAICH [3], Wajih GAFSI [2], Lassaad WALHA [2], Mohamed HADDAR [2]

[1] Laboratory of Mechanics of Normandy (LMN), National Institute of Applied Sciences of Rouen, Rouen, France.

[2] Laboratory of Mechanics, Modeling and Manufacturing (LA2MP), Mechanical Engineering Department, National School of Engineers of Sfax, Sfax, Tunisia.

3 Institute of Thermal, Mechanic, Materials (ITheMM); University of Reims Champagne-Ardenne, EiSINe, Campus Sup Ardenne, France.

Abstract

This paper presents an efficient numerical investigation of a PCM-based heat sink for the purpose of thermal management, that leads to determine its optimal configuration. This study is based on experimental results, where a comparison between heat sink with and without phase change material (PCM) was carried out. Furthermore, a detailed analysis of various parameters' effects of the studied PCM-based heat sink in relation with geometry, boundary conditions and material parameters were studied. Numerical results show that n-Eicosane increases clearly the thermal performance of the studied cooling system, comparing with other studied PCMs. In addition, increasing the volume fraction of PCM leads to delay the latent heating phase and then increase the thermal management behavior. Also, as expected, increasing the input power level leads to increase the melting rate of PCM. The parametric analysis lead finally to define an optimal design with an efficient thermal performance, for both charging and discharging phases.

Keywords: Phase Change Materials; Finned heat sink; Cooling Mechatronic Components; Heat flux; Finite Elements Analysis; Thermal management.

1 Introduction

In the last few decades, thermal management of heat transfer, particularly in the field of mechatronics, presents a complex problem that has been of great attentions for researchers in several domains, such as laptops [1], smartphones [2] [3], digital video cameras, automobile and even planes [4] [5] [6] etc.

Increasing the development of electronic packaging technology means that components sizes are getting smaller. To this end, several issues can be detected such as high heat flux generated by the electronic components. Then, an efficient thermal management is needed to avoid its failure or malfunction.

In most cases, standard cooling methods would not be sufficient. In fact, due to some limitations such as limited thermal conductivity of air and cooling system materials also due to spaces limitation, the input heat load produced during continuous operation over long periods cannot be evacuated. In this context, PCM-based heat sinks are among the best-known passive cooling systems. This technology is very advantageous and necessary to increase its performance.

In the literature, several methods of reducing the temperature by heat dissipation from active devices are developed [7] [8] [9]. Some of these cooling systems are based on phase change materials (PCMs) [10] [11] [12] [13] [14] [15] [16]. In fact, it has been demonstrated that this new technology of cooling systems is more efficient especially in cases of devices which operate intermittently for short periods [11].

Most PCMs are characterized by their high latent heat of fusion which means a high ability to store energy. The heat dissipated by the component is absorbed by PCM and then released back later, benefiting from its thermo-physical properties.

The selection of PCMs for a specific application is based on the maximum operating temperature of the device, i.e., the melting temperature of the PCM should be lower than the maximum operating temperature of the component. In general, the global maximum temperature allowed of such a component should not exceed 85°C to 120°C [17].

Generally, Copper and aluminum are the most used metals to improve the overall thermal response of the heat sink. Despite the fact that the value of the thermal conductivity of aluminum is less than copper, its use is more favorable. In fact, it is characterized by its low density, its corrosion resistance and also its easy machinability.

In [18], authors aim to evaluate thermal storage rate of a PCM comparing with that of a PCM–metal foam composite for multi-layered parallel-plate thermal storage device. This study proves that the heat transfer enhancement with PCM-metal foams is required for thermal storage process. Also, thermal transport in microchannels partially filled with micro-porous media involving flow inertia, flow/thermal slips, thermal non-equilibrium and thermal asymmetry, was conducted in [19] by Xi H.J.

Nazzi Ehms et al. [20] present a review on fixed grid numerical models for solidification and melting of PCMs. This study demonstrates that “enthalpy–porosity” is the most common numerical model used in PCM studies. Additionally, a new basic approach was proposed in order to determine the computing performance in transient numerical simulations. Moreover, in [21], authors present a numerical analysis on phase change materials (PCM) where the solidification process of erythritol in spheres was studied.

To quantify the heat transfer performance of a PCM-based plate fin matrix, Baby and Balaji [11] were conducted an experimental study under constant and intermittent heat loads. An experimental comparison of the thermal performance of plate fin heat sink matrix filled with and without PCM at different power settings was proposed.

The aim of this paper is to propose an optimal design of the studied cooling system, based on a numerical investigation of PCM-based heat sink. The efficiency of the proposed model is verified numerically based on experimental data presented by Baby and Balaji [11].

The studied cooling system is composed of plate fin heat sink matrix made of aluminum. In this case, the n-Eicosane is used as a PCM to improve the thermal storage behavior of the proposed model. Also, to have a better results accuracy, all sides of the cooling system are supposed adiabatic.

A parametrical study is then carried out in this paper, where four cases are studied. The main objective is to compare the thermal performance when changing (i) PCM material (ii) input power level (iii) PCM volume fraction and (iv) heat sink geometry. For each case, the thermal performance comparison is based on the study of two heat flux excitation phases: charging phase and discharging phase. An optimal design of a cooling system is then proposed. This design presents an efficient thermal management behavior.

2 Finite element analysis of the cooling system

2.1 Studied model description

The phase change material-based heat sink was proposed by Baby and Balaji [11]. Figure 1 shows the studied model of the heat sink. It is made from aluminum and composed of plate fin-heat sink matrix. There are 4 x 4 enclosures in the studied heat sink filled with n-Eicosane as a PCM.

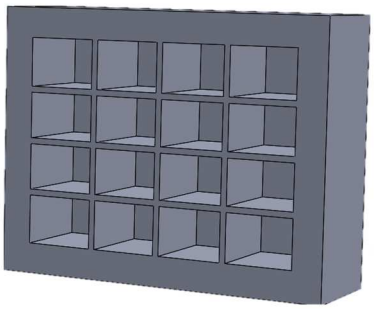

Figure 1. Plate fin matrix heat sink model

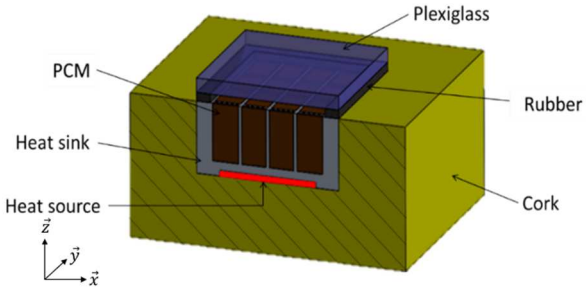

Figure 2. Assembly model cut

All sides of heat sink were insulated with cork, except the top surface, as shown in figure 2.The upper part of the heat sink was occupied for a plexiglass sheet. A rubber packing was

putted between the heat sink and the plexiglass sheet. In order to reproduce the heat generated by the electronic component, a plate heater was placed at the base of the heat sink.

2.2 Mathematical description of heat transfer and PCM behavior

The heat generated by the heat source is transmitted to the surface of heat sink by conduction. A portion of the heat stored in the heat sink is evacuated into the ambient air by natural convection and radiation. The heat exchange coefficient h is then between 10 and 25 $[W/m^2K]$. It is assumed that the heat is transferred by conduction between the base, the PCM, the fins as well as the end walls.

The energy absorbed by the PCM causes its transformation from solid to liquid, and the dissipated energy causes its transformation of the liquid to solid. It is assumed that the thermo-physical properties of PCM are independent of temperature.

The following three-dimensional conservation equations for mass, momentum and energy can be written as follows:

- **Mass conservation:**

$$\frac{\partial \rho}{\partial t} + \frac{\partial (\rho u)}{\partial x} + \frac{\partial (\rho v)}{\partial y} + \frac{\partial (\rho w)}{\partial z} = 0 \tag{1}$$

Note that the liquid PCM is considered as incompressible Newtonian fluid (the density of PCM ρ does not change for any fluid particle $\frac{\partial \rho}{\partial t} = 0$). The continuity equation is reduced to:

$$\frac{\partial u}{\partial x} + \frac{\partial v}{\partial y} + \frac{\partial w}{\partial z} = 0 \tag{2}$$

Where, u, v and w are the velocity components in x, y and z directions, respectively.

- **Momentum conservation:**

$$\rho\left(\frac{\partial u}{\partial t} + \frac{\partial u^2}{\partial x} + \frac{\partial (uv)}{\partial y} + \frac{\partial (uw)}{\partial z}\right) = -\frac{\partial P}{\partial x} + \mu\left[\frac{\partial^2 u}{\partial x^2} + \frac{\partial^2 u}{\partial y^2} + \frac{\partial^2 u}{\partial z^2}\right] + S.u \tag{3}$$

$$\rho\left(\frac{\partial v}{\partial t} + \frac{\partial (uv)}{\partial x} + \frac{\partial v^2}{\partial y} + \frac{\partial (vw)}{\partial z}\right) = -\frac{\partial P}{\partial y} + \mu\left[\frac{\partial^2 v}{\partial x^2} + \frac{\partial^2 v}{\partial y^2} + \frac{\partial^2 v}{\partial z^2}\right] + S.v \tag{4}$$

$$\rho\left(\frac{\partial w}{\partial t} + \frac{\partial (uw)}{\partial x} + \frac{\partial (vw)}{\partial y} + \frac{\partial w^2}{\partial z}\right) = -\frac{\partial P}{\partial z} + \mu\left[\frac{\partial^2 w}{\partial x^2} + \frac{\partial^2 w}{\partial y^2} + \frac{\partial^2 w}{\partial z^2}\right] - \rho g \alpha_w (T - T_{sol}) + S.w \tag{5}$$

where, P presents the pressure, μ is the dynamic viscosity, g is the gravitational acceleration, α_w is the thermal expansion coefficient and t is the time. As mentioned in Eq. (5), the

Boussinesq approximation is adopted by adding $\rho g \alpha_w (T - T_{sol})$ term, due to the gravitational acceleration direction in the negative *z*-direction.

The source term *S* in momentum equations can be written as follows:

$$S = \frac{(1 - \beta_{PCM})^2}{({\beta_{PCM}}^3 + \varepsilon)} A_m \tag{6}$$

where parameter ε is a small positive number ($\varepsilon = 10^{-10}$), used to avoid division by zero. The constant A_m refers to the consecutive number in the mushy region. As recommended in several studies [22] [23] [24], the value of $A_m = 10^5$ is considered in present study.

The PCM liquid fraction β_{PCM} is defined as the liquid quantity relative to the total volume of the PCM [25] [26], which can be written as below:

$$\beta_{PCM} = \begin{cases} 0 & if \quad T < T_{sol} \\ \dfrac{T - T_{sol}}{T_{liq} - T_{sol}} & if \quad T_{sol} < T < T_{liq} \\ 1 & if \quad T > T_{liq} \end{cases} \tag{7}$$

The fraction of the liquid state material is estimated to be 0 for a total solid, 1 for a total liquid and between 0 and 1 for the latent phase of PCM.

- **Energy conservation:**

$$\rho C_P \left(\frac{\partial T}{\partial t} + u\frac{\partial T}{\partial x} + v\frac{\partial T}{\partial y} + w\frac{\partial T}{\partial z}\right) = \lambda \left(\frac{\partial^2 T}{\partial x^2} + \frac{\partial^2 T}{\partial y^2} + \frac{\partial^2 T}{\partial z^2}\right) + S_h \tag{8}$$

Where, C_P is the specific heat at constant pressure and S_h is the energy source term. It represents the latent heat storage due to melting and it can be expressed as follows:

$$S_h = -\frac{\partial(\rho \Delta H)}{\partial t} \tag{9}$$

The total enthalpy of PCM can be written as the sum of the specific enthalpy h_s and the latent heat ΔH:

$$H = h_s + \Delta H \tag{10}$$

Which the specific enthalpy h_s is defined as follows:

$$h_s = h_{s,ref} + \int_{T_{ref}}^{T} C_p dT \tag{11}$$

Accordingly, the latent heat ΔH can be written in terms as the product of the latent heat of fusion L_f by the liquid fraction:

$$\Delta H = \beta_{PCM} . L_f \tag{12}$$

So, the total enthalpy of PCM H can be defined as follows:

$$H = h_{s,ref} + \int_{T_{ref}}^{T} C_p dT + \beta_{PCM}.L_f \quad (13)$$

For this simulation, the used mathematical models can be found in Wang and Yang [22, 23] Shatikian et al. [24] and Nayak et al. [27]. They investigated the performance of heat transfer of PCM in internal fins.

2.3 Geometry and boundary conditions

The detailed geometry of heat sink is presented in figure 3. The plate fin heat sink is made from aluminum of overall dimensions 80 x 62 mm² base with a height of 25 mm and a side wall thickness of 7 mm. The PCM is filled in the enclosures to a height of 20 mm in the studied heat sink. The material properties of each component of the assembly are mentioned in table 1.

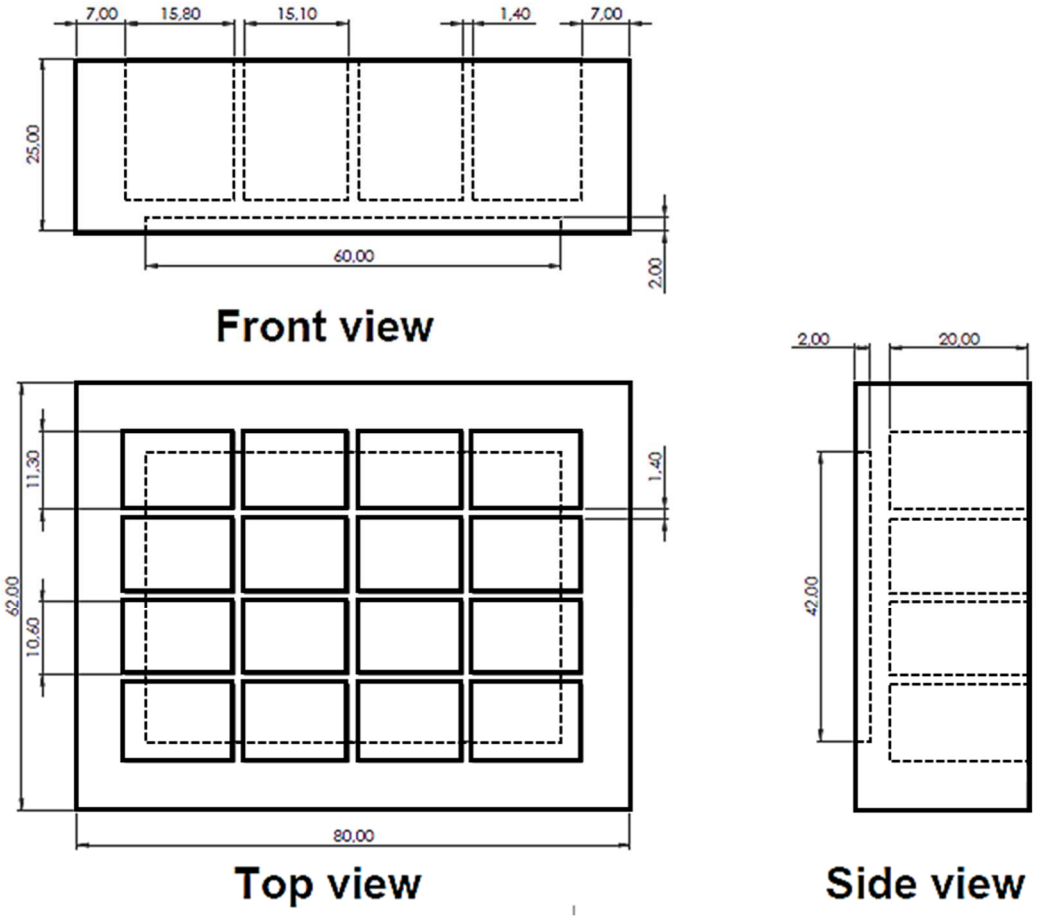

Figure 3. Heat sink geometry

Numerically, the input power is modeled as a heat flux to mimic the plate heater used experimentally. It is applied on an enclosure provided at the base of heat sink of overall dimensions of 60 x 42 x 2 mm^3.

Table 1. Materials thermophysical properties

Material	Thermal conductivity $(W/m.K)$	Specific heat $(kJ/kg.K)$	Latent heat (kJ/kg)	Solidification point $(°C)$	Melting point $(°C)$	Density (kg/m^3)
Aluminum	202.4	0.87	-	-	606.4	2719
Cork	0.045	0.35	-	-		120
Caoutchouc	0,16	0.001	-	-		1190
Plexiglass	0,19	1.47	-	-		1190
n-Eicosane	0.39 (s) 0.157 (l)	1.9 (s) 2.2 (l)	237.4	35.5	36.5	810 (s) 770 (l)

To model the phase transition effect in the PCM-based heat sink, an "enthalpy-porosity" method is adopted. To create the PCM-based finned heat sink model, the following hypotheses were taken in the present numerical study:

- The heat sink material is isotropic and homogeneous.
- There is a local thermal equilibrium between liquid PCM and fins.
- Assuming that the thermophysical properties of the fins and the PCM remain constant whatever the phase and the temperature.

Note that only the melting temperature value of the n-Eicosane was identified in [11]. However, for a numerical modeling preference, a temperature range of the latent heating phase, $\Delta T = T_{liq} - T_{sol} = 1°C$ has been considered [28]. Here, T_{sol} and T_{liq} represent respectively the solidification and the melting temperature of the PCM (see table 1).

Exterior walls of the cork are exposed to natural convection and radiation. Moreover, the phase change phenomenon takes place inside the PCM-based heat sink in transient mode. It should be mentioned that the lateral heat sink walls are supposed adiabatic. In fact, these walls are insulated by cork which has a low thermal conductivity (see table 1).

To solve the governing equations in this case, the applied boundary conditions are as follows:

- Initial condition

  $t = 0$, $T = T_{amb} = 27°C$, $\beta_{PCM} = 0$

In other word, at $t=0$ the entire assembly is exposed to an ambient temperature T_{amb} and the PCM is in its solid phase.

- Heat flux provided to the input power enclosure:

$$-\lambda \frac{\partial T}{\partial x}\Big|_{\substack{x=10\to70 \\ y=10\to52 \\ z=2}} = -\lambda \frac{\partial T}{\partial y}\Big|_{\substack{x=10\to70 \\ y=10\to52 \\ z=2}} = Q$$

2.4 Preliminary results and discussions

To study the PCM based heat sink, ANSYS Workbench v17.2 is used as a Finite Element (FE) computing software. The finite element model of the heat sink is presented in figure 4. The studied cooling system (without PCM) was discretized into a total number of 49449 10-node tetrahedral thermal elements (figure 4 (a)).

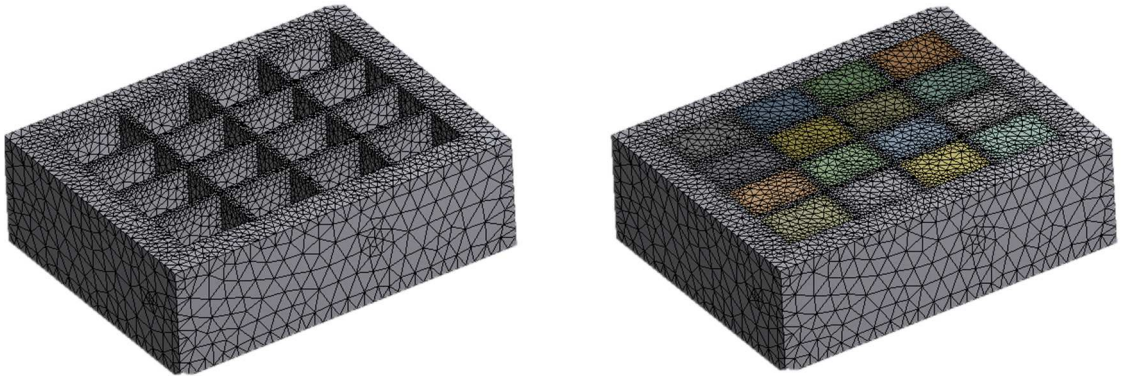

(a) (b)

Figure 4. Mesh of the heat sink: (a) without PCM (b) with PCM

Six different mesh size are investigated. In figure 5, the maximum reached temperature convergency is investigated (blue curve). The total computing time for each mesh configuration is presented by the orange curve.

From these results, and for a best compromise between accuracy and cost, the mesh of 49449 elements is selected in this numerical study for more simulations.

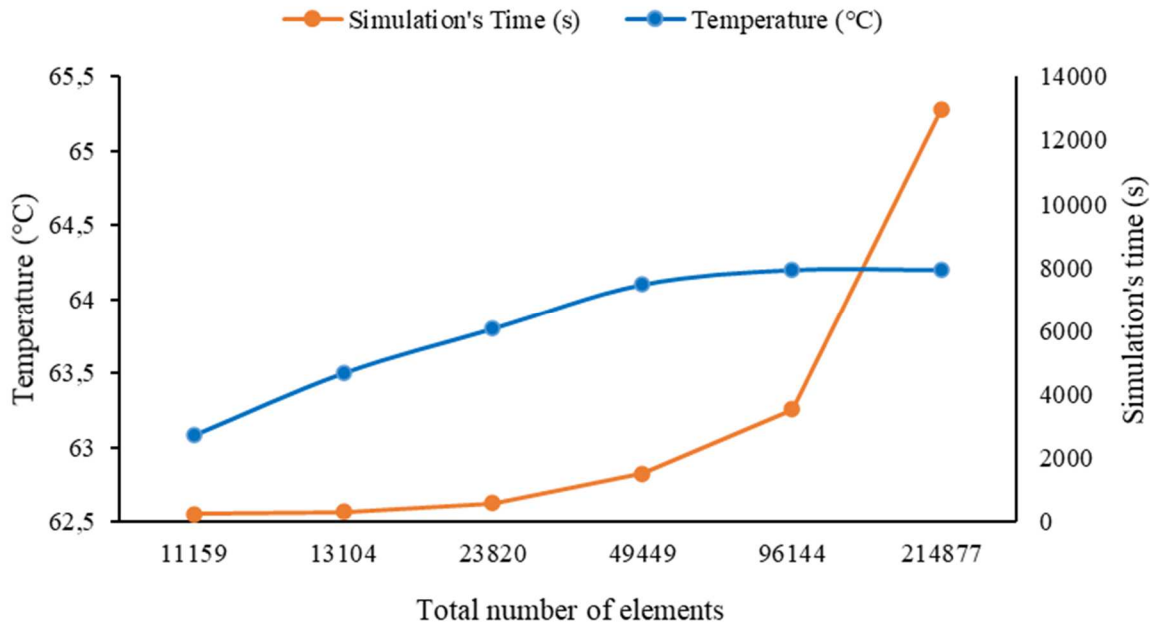

Figure 5. Convergence study

The total number of elements is about 109485 elements for heat sink model fulfilled with PCM (figure 4 (b)). Note that, a mesh refining is used at the contact areas of PCM and heat sink. This refining leads to guarantee a better accuracy of results.

Figure 6 shows the temperature variation at the base of the HS, as a function of time. Note that the red curve and the blue curve present respectively the with-PCM and without-PCM configurations. The temperature-time profile can be divided into two distinct parts: charging phase and discharging phase.

For the charging phase, it can be clearly seen that, in the without–PCM configuration, the temperature increases from an ambient temperature (27°C) to the steady state temperature (about 65°C). Initially, the temperature increases in a linear way, then its rate decreases with time.

However, benefiting from its thermo-physical properties, PCM has delay the increase of the temperature compared with that without–PCM. Then, as it can be observed, for the charging phase, the red curve can be divided into three distinct regions: solid phase, latent heating phase and liquid phase of PCM.

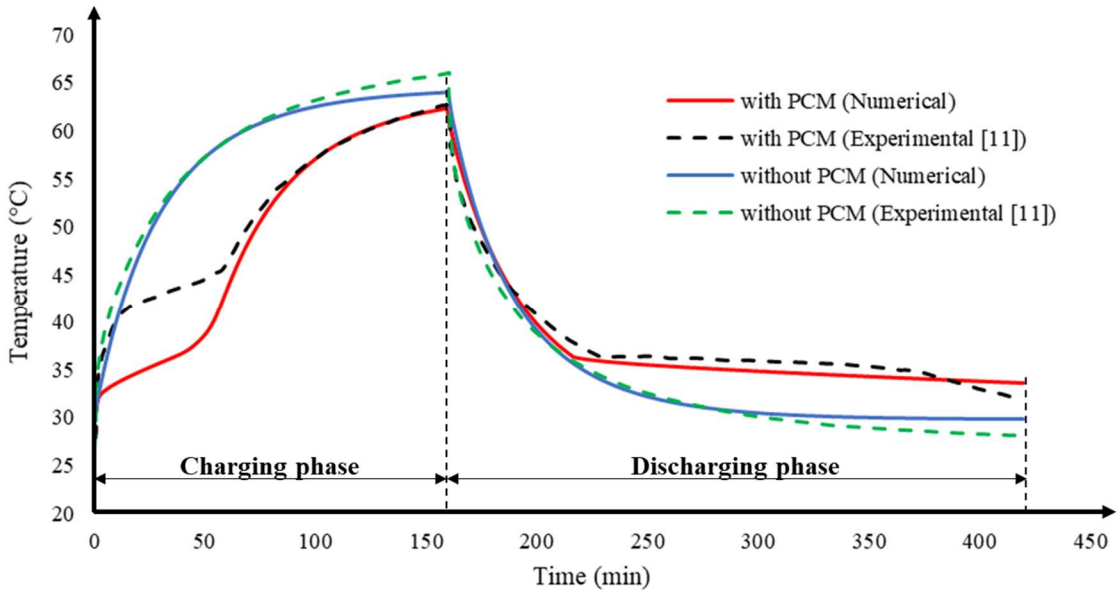

Figure 6. Temperature profile at the heat sink base under Q=7W

Another observation that can be made from figure 6 is that the numerical simulation results on case temperatures compare reasonably well with the experimental data. Note that discontinues black and green curves present respectively experimental temperature profiles for both with and without PCM configurations [11].

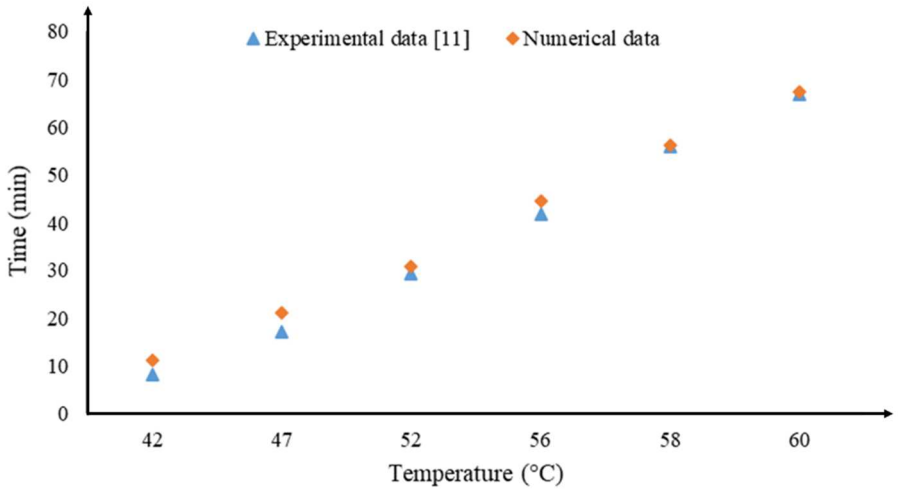

(a)

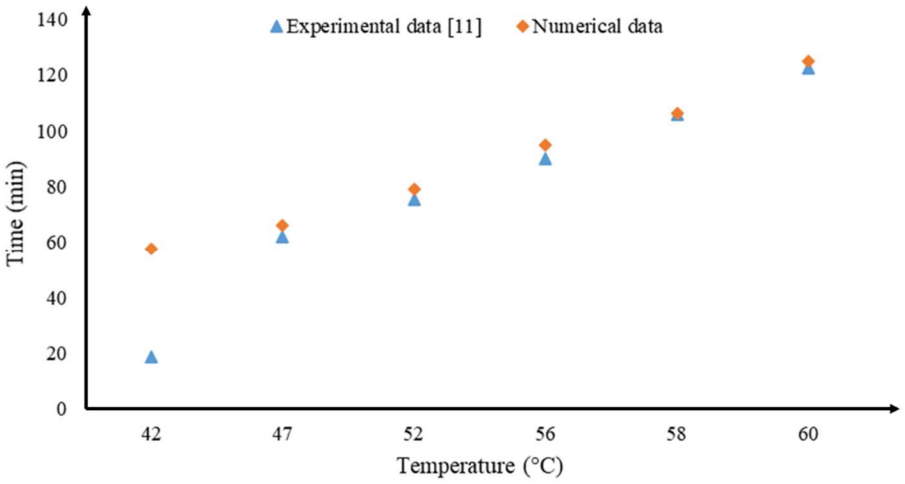

(b)

Figure 7. Time to reach specific temperatures: (a) without PCM (b) with PCM

Figure 7 presents a comparison of numerical model with experimental data for both configurations (with/without PCM). Each point presents the time taken to reach different set point temperatures measured at the base of the heat sink. Note that the blue triangles indicate the experimental results and the orange squares represent the numerical results. It should be noted that experimental data are obtained referring to Baby et al. study [11].

For these set points, a maximum observed error between numerical and experimental results is about four minutes in both cases, except for the first set point of figure 7 (b) (about 40 min). In fact, referring to figure 6, the first liquid drops appear nearly at T = 42°C, while theoretically the PCM melting temperature is about 36.5°C. Otherwise, this condition is validated numerically.

3 Parameters influence

In this section, the thermal behavior of PCM-based finned heat sink is performed. Then, its sensitivity to the material properties and geometric parameters is highlighted. Finally, an optimal model in the studied parameters domain was proposed in term of thermal management behavior.

3.1 PCM selection

The melting temperature is one of the most important PCM thermophysical properties for the cooling of mechatronic components. In fact, PCM selection is based on temperature ranges. Here, its solidification temperature must be higher than the ambient temperature and its melting temperature must be lower than the steady state temperature. In [29], authors aim to study the effect of using three PCMs (salt hydrate, paraffin and milk fat) as thermal regulators for cooling of electronic components. Since the solidification temperature of the milk fat (about 10°C) is lower than the ambient temperature, it is not considered in this study. Thus, salt hydrate and paraffin are then compared with the n-Eicosane to study its thermal behavior. The thermo-physical properties of each studied PCM material are presented in table 2.

Table 2. PCMs thermo-physical properties

Material	Thermal conductivity $(W/m.K)$	Specific heat $(kJ/kg.K)$	Latent heat (kJ/kg)	Solidification point $(°C)$	Melting point $(°C)$	Density (kg/m^3)
Salt hydrate [29]	0.6	2	200	27	32	1500
n-Eicosane	0.39 (s) 0.157 (l)	1.9 (s) 2.2 (l)	237.4	35.5	36.5	810 (s) 770 (l)
Paraffin [29]	0.20	2	140	38	43	802

In addition to n-Eicosane, paraffin and salt hydrate are used as PCM material for the studied cooling system. In fact, salt hydrate is characterized by its higher conductivity and negligible volume changing during latent phase. Also, it is a low-cost material comparing with other PCMs. However, it has various problems like: corrosion to metals [30, 31], chemical instability [32] and lower thermal stability [30, 33] .

For the paraffin, it has approximatively the same heat capacity as the salt hydrate. However, it is characterized by a lower thermal energy storage comparing with other studied PCMs.

Besides, the paraffin has a lower conductivity and a lower density, which requires a larger containment size then it occupies more volume which reduces the storage energy density.

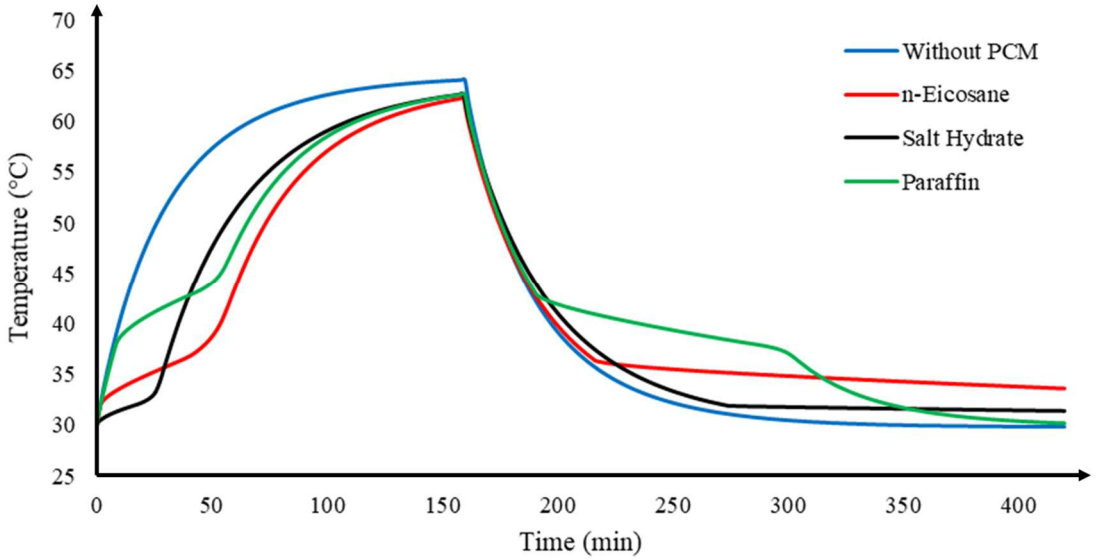

Figure 8. Melting and cooling temperature profile for three PCMs

Figure 8 compares the thermal performance of the PCM-based heat sink for four cases: one is for the heat sink without PCM (blue curve) and the rest are for heat sink filled with PCMs mentioned in table 2. Note that the input power in this study is about 7W.

When charging, we assume that the salt hydrate maintained lower temperature for first few minutes comparing with the other PCMs. However, it takes lesser time to be totally melted. As a consequence, the salt hydrate will not be able to store more energy dissipated by the component.

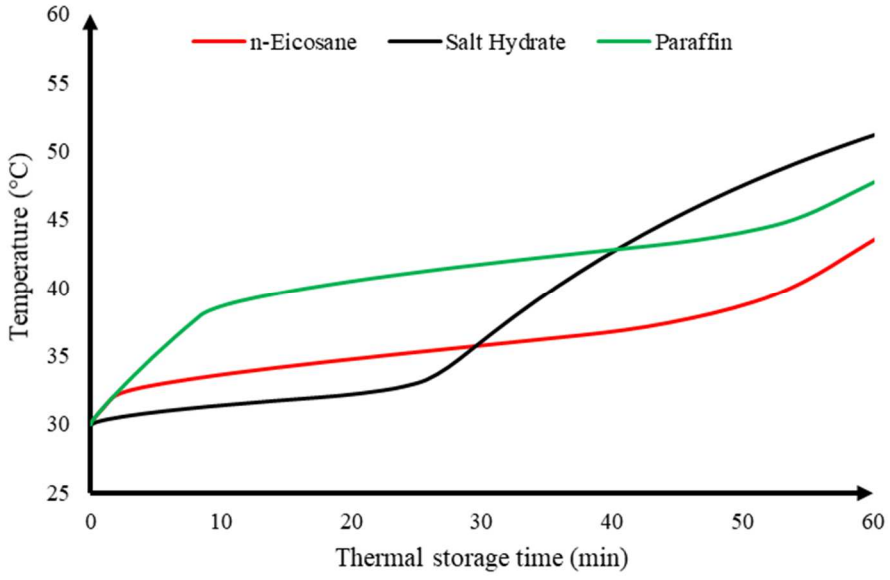

Figure 9 : Latent process for three PCMs (charging phase)

It should be mentioned that salt hydrate starts melting at T=27°C while the ambient temperature that the electronic device operates normally is about 29°C. Therefore, the salt hydrate remains partially melted in electronic components even before the departure of its use. Then, some of storage energy is not explored. So, the salt hydrate is not required as a PCM for this study.

Furthermore, we note that the n-Eicosane latent phase last longer comparing to paraffin. Also, the n-Eicosane melting temperature is about 36.5°C against 43°C for paraffin. Then, at each time of the charging phase, the measured temperature at the base is always lower when using n-Eicosane as a PCM (see figure 9).

3.2 Power level

Figure 10 shows the temperature – time history measured at heat sink base at different power levels: 2, 5, 7 and 10W. Note that the used PCM in this section is the n-Eicosane. This choice is based on the study presented in the previous section.

It can be seen that the temperature of the heat sink increases when the heat power increase. For example, the temperature at t=160 min for a power level of 10W is about 76°C against 62°C and 50°C for input power of 7W and 5W respectively. Furthermore, for an input of 2W (black curve), the PCM is not fully melted, even at the end of the charging phase.

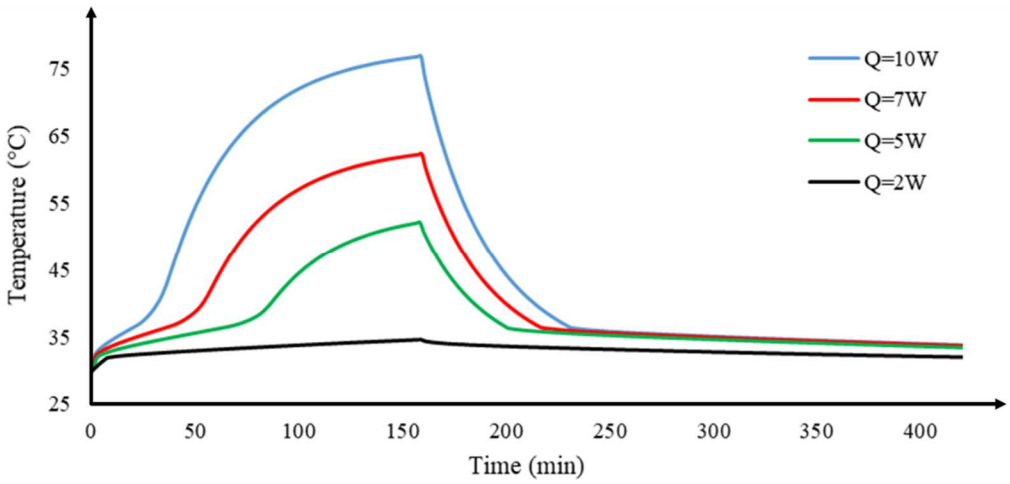

Figure 10. Variation of the temperature profile under four power levels

One interesting observation is that there are different melting durations, as shown in figure 10. The time taken for the latent heating phase increases as the heating power is decreased. For the 5W heat input, the PCM is completely melted only after 75 min, but it ends within 30 min for a power input of 10W.

3.3 PCM volume fraction

In the current section, we define the volume fraction of the PCM δ, as the ratio of the volume occupied by PCM to the total volume of the heat-sink's enclosures. The studied volume fractions are from 0% (without PCM) to 100 % (heat sink fully filled with PCM) with 25% steps.

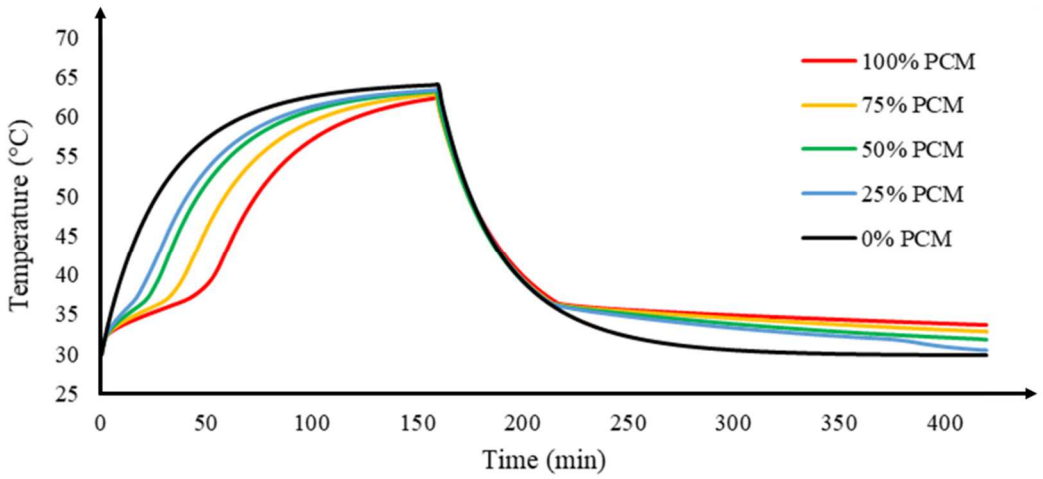

Figure 11. Variation of the temperature profile for different volume fraction of PCM

Figure 11 presents the temperature-time profile for the different volume fractions. It can be clearly seen that the increase of PCM volume fraction leads to delay the PCM total melting time and then increases the ability to store more dissipated heat.

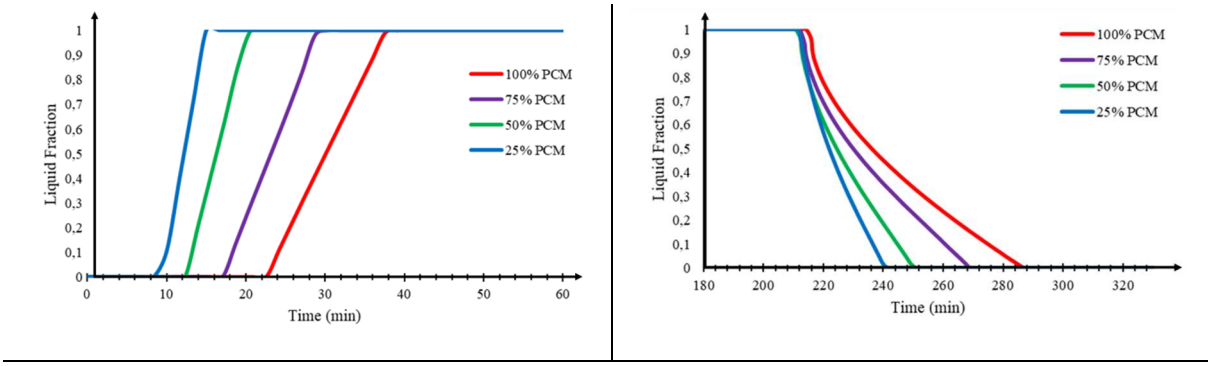

Figure 12. Liquid fraction versus time for different PCM volume rate

The variation of PCM liquid fraction for different volume rate is investigated in figure 12, for both charging and discharging phase. This figure shows the benefits of using PCM in energy storage capability. Accordingly, the fulfilled heat sink presents the best thermal management efficiency for the charging phase.

For the discharging phase, as shown in figure 12 (b), it can be noted that more PCM leads to heat dissipation issues. In fact, it takes more time to complete the liquid-solid phase change process. This is caused by the fact that, the n-Eicosane has a very low thermal conductivity while aluminum fins have a thermal conductivity of 202.4 [W/m K]. This makes the PCM behaves like an insulator comparing with the fins which are a good heat conductor.

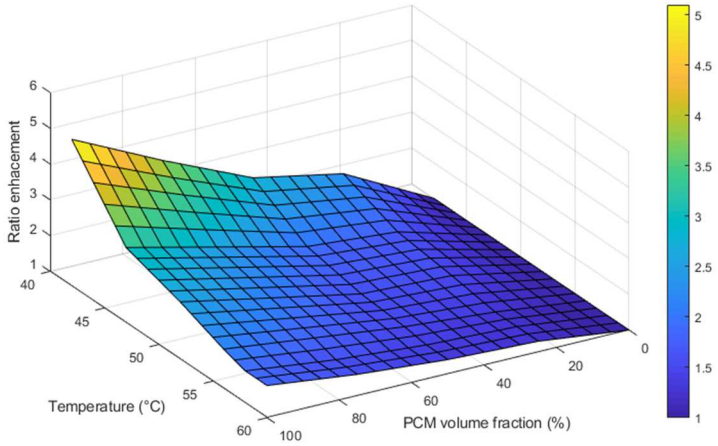

Figure 13. PCM enhancement ratio of the heat sink matrix for different temperatures

In order to verify the efficiency of studied model, an enhancement ratio is defined as the ratio of the time taken by the PCM-based heat sink to the time taken by a heat sink without PCM, at each temperature. It can be mathematically written as follow:

$$E_{PCM}(T) = \frac{t(T,\delta)}{t(T,\delta = 0)} \tag{14}$$

Figure 13 presents the enhancement ratio in terms of temperature and PCM volume fraction. As shown, the increase of the volume fraction results in higher enhancement ratio, particularly for low temperature.

3.4 Cavities number

Let's consider now four configurations of heat sinks presented in figure 14. The used plate fin matrices are respectively 2x2, 3x3, 4x4 and 6x6. Note that the config.4 of figure 14.(c) is the same model studied previously.

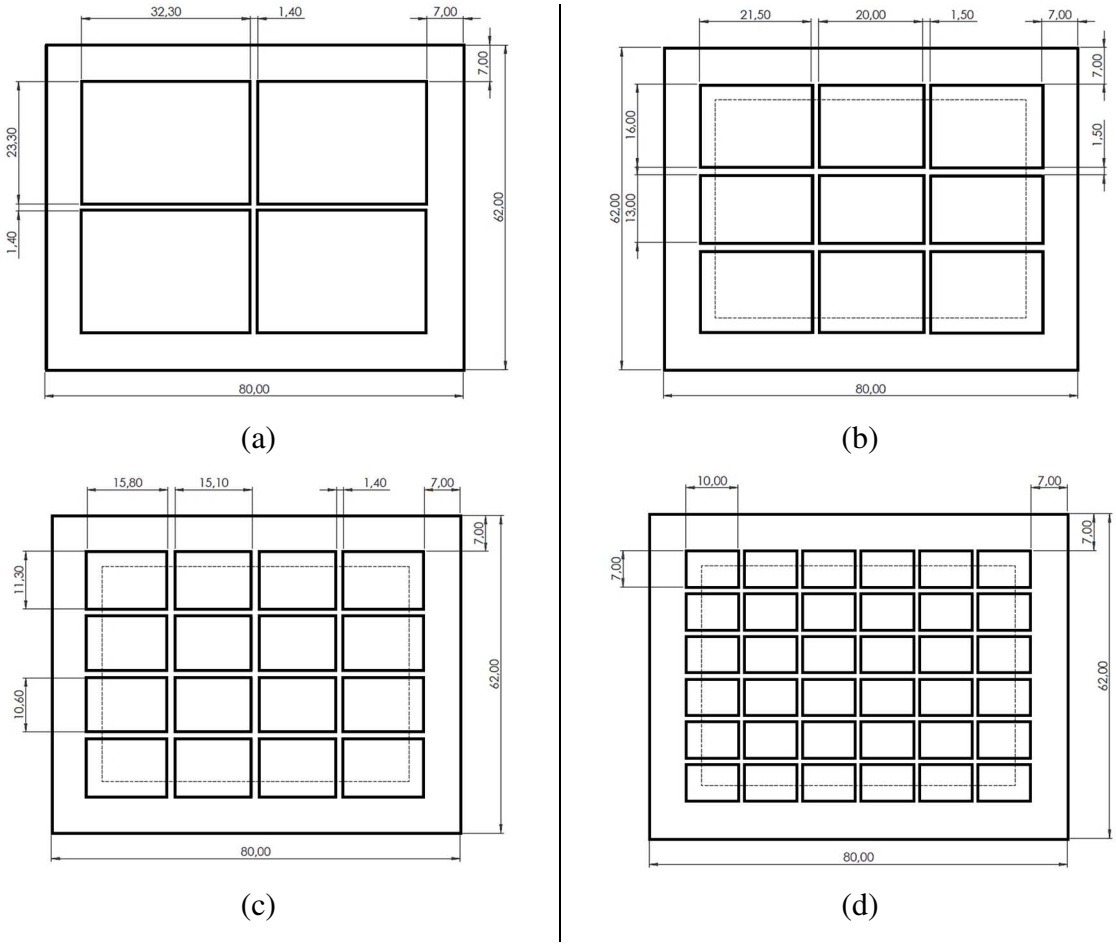

Figure 14. Detailed set up of the different configuration of heat sink

(a) config.1: 2x2 (b) config.2: 3x3 (c) config.3: 4x4 (d) config.4: 6x6

Figure 15 presents the resulted temperature-time profile for each configuration. It can be clearly seen that the first configuration presents the best thermal management performance in term of maximum reached temperature.

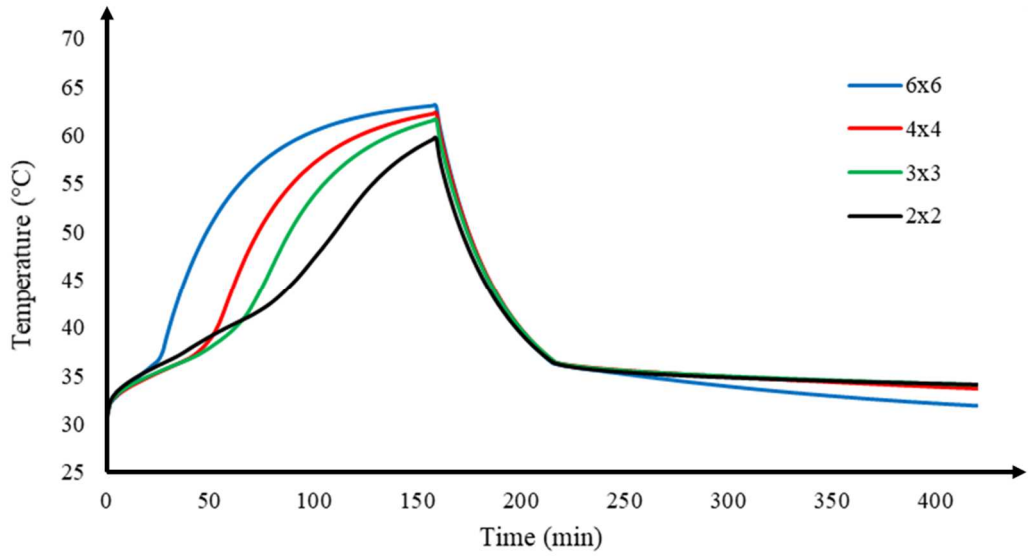

Figure 15.Variation of the temperature profile for different heat sink Geometry

We note that decreasing the enclosures number delay the latent heating phase and then more ability to store energy in the charging phase.

Times to reach some set point temperatures for the proposed configurations are studied in figure 16. Throughout the solid phase, as presented by the blue curve (33°C), the time to reach such temperatures is similar for each configuration. So, we conclude that, in this phase, the enclosures number has no effect on temperature evolution. However, after PCM melting, the time to reach a set points temperature increases when the enclosures number decreases.

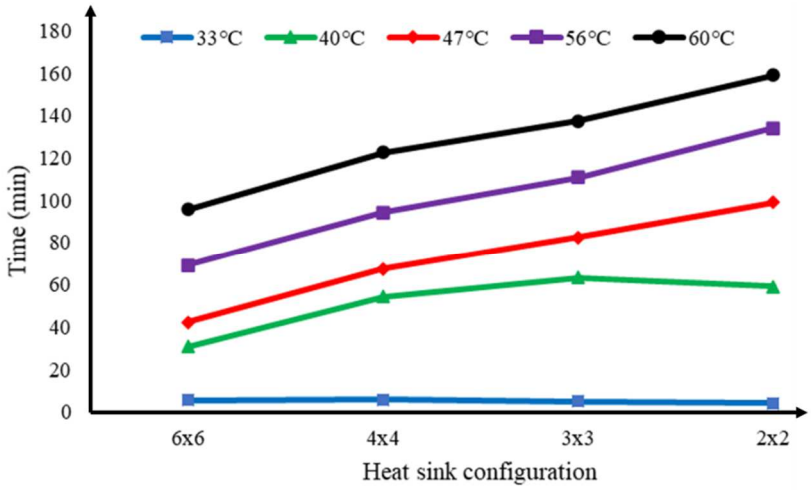

Figure 16. Time to reach set points temperature for different heat sink configurations

For the discharging phase, the 6x6 configuration has more ability to dissipate stored heat comparing with other configurations. This can be explained by the fact that more fins mean more aluminum volume rate. In fact, as shown in table 1, the aluminum thermal conductivity is very important than the thermal conductivity of n-Eicosane. This makes the fins good heat conductors while the PCM behaves almost like an insulator.

3.5 Adopted parameters for the studied cooling system

The parametric analysis lead not only to study the thermal behavior of cooling system of mechatronics components, but also to define an optimal design able to provide a minimal reached temperature for both charging and discharging phases. Various parameters were studied in order to determine the more effective heat transfer mechanism.

From the parametrical study, it can be concluded that n-Eicosane presents more ability to store energy comparing with other PCMs. Also, δ =1 (fully filled enclosures) presents the optimal PCM volume fraction for the charging phase. In addition, heat sink with 2x2 enclosures presents an increase in the latent heating phase period and then delay the maximum reached temperature. An experimental study is needed in order to improve the

founded numerical results and to identify all studied physical parameters of the proposed model.

4 Conclusion

In the present paper, a finite element analysis of a cooling system for mechatronic components were conducted to quantify the heat transfer performance of a PCM-based heat sink. the efficiency of the numerical results was verified referring to experimental data of Baby and Balaji illustrated in Ref. [11]. Furthermore, the temperature evolution of the heat sink was elucidated for both charging and discharging process.

The presented results show the impact of four parameters (PCM material; input power level; PCM volume fraction and heat sink geometry) on the thermal management behavior of the proposed cooling system. First, we observed that n-Eicosane have more ability to store thermal energy comparing with other studied PCMs. Also, to have the optimal thermal management behavior, heat sinks enclosures should be fulfilled with PCM.

The total latent heating phase process proved to be augmented by the decrease of the input power level. Otherwise, increasing the input heat level has similar effect on the maximum reached temperature. It is also possible to approve that the main influence of the heat sink enclosures configuration, as this defines the amount of PCM in the cooling system and consequently the amount of energy stored. As a result, in this study, we conclude that the heat sink of 2x2 enclosures presents an increase in the latent heating phase period.

Obtained results confirm the benefits of using the FE analysis for cooling system with complex behavior. This study led to propose an optimal design of the cooling system. This model presents an efficient thermal management performance.

The proposed model is of direct interest to design a PCM-based cooling system. The obtained results are encouraging, considering the literature about cooling systems. This study creates one more step to reinforce methods for studying PCM-based cooling system behavior.

5 References

[1] N. Leoni and C. H. Amon, "Bayesian surrogates for integrating numerical, analytical, and experimental data: application to inverse heat transfer in wearable computers," *IEEE Transactions on Components and Packaging Technologies,* vol. 23, no. 1, pp. 23-32, 2000.

[2] S. Fok, W. Shen and F. Tan, "Cooling of portable hand-held electronic devices using phase changematerials in finned heat sinks," *International Journal of Thermal Sciences,*

vol. 49, no. 1, pp. 109-117, 2010.

[3] R. Kandasamy, X. Wang and A. Mujumdar, "Application of phase change materials in thermalmanagement of electronics," *Applied Thermal Engineering,* vol. 27, no. 17-18, pp. 2822-2832, 2007.

[4] W. R. Humphries and E. I. Griggs, "A design handbook for phase change thermal control and energy storage devices," *NASA STI/recon technical report,* no. 78, 1977.

[5] A. Fossett, M. Maguire, A. Kudirka, F. Mills and D. Brown, "Avionics passive cooling with microencapsulated phase change materials," *Journal of Electronic Packaging,* vol. 120, no. 3, pp. 238-242, 1998.

[6] D. Pal and Y. Joshi, "Thermal management of an avionics module using solid-liquid phase-change materials," *Journal of Thermophysics and Heat Transfer,* vol. 12, no. 2, pp. 256-262, 1998.

[7] A. B. Etemoglu, "A brief survey and economical analysis of air cooling for electronic equipments," *International communications in heat and mass transfer,* vol. 34, no. 1, p. 103–113, 2007.

[8] R. Grimes, E. Walsh and P. Walsh, "Active cooling of a mobile phone handset," *Applied Thermal Engineering,* vol. 30, no. 16, p. 2363–2369, 2010.

[9] Z. Luo, H. Cho, X. Luo and K. I. Cho, "System thermal analysis for mobile phone," *Applied Thermal Engineering,* vol. 28, no. 14-15, p. 1889–1895, 2008.

[10] K. Chintakrinda, R. Weinstein and A. Fleischer, "A direct comparison of three different material enhancement methods on the transient thermal response of paraffin phase change material exposed to high heat fluxes," *International Journal of Thermal Sciences,* vol. 50, no. 9, p. 2011, 1639-1647.

[11] R. Baby and C. Balaji, "Thermal performance of a PCM heat sink under different heat loads: an experimental study," *International Journal of Thermal Sciences,* vol. 79, pp. 240-249, 2014.

[12] D. Zhou and C. Y. Zhao, "Experimental investigations on heat transfer in phase change materials (PCMs) embedded in porous materials," *Applied Thermal Engineering,* vol. 31, no. 5, pp. 970-977, 2011.

[13] Y. Tian and C. Y. Zhao, "A numerical investigation of heat transfer in phase change materials (PCMs) embedded in porous metals," *Energy,* vol. 36, no. 9, pp. 5539-5546, 2011.

[14] I. Mjallal, H. Farhat, M. Hammoud, S. Ali and I. Assi, "Improving the Cooling Efficiency of Heat Sinks through the Use of Different Types of Phase Change Materials," *Technologies,* vol. 6, no. 1, p. 5, 2018.

[15] B. Debich, A. Yaich, A. Elhami, W. Gafsi, L. Walha and M. Haddar, " Coupling PCM-based Heat Sinks finite elements model for mechatronic devices with Design

Optimization procedure," *IEEE 6th International Conference on Optimization and Applications (ICOA),* pp. 1-4, 2020.

[16] S. K. Saha and P. Dutta, "Role of Melt Convection on Optimization of PCM-Based Heat Sink Under Cyclic Heat Load," *Heat Transfer Engineering,* vol. 34, no. 11-12, pp. 950-958, 2013.

[17] A. Coskun, D. Atienza, T. Rosing, T. Brunschwiler and B. Michel, "Energy-efficient variable-flow liquid cooling in 3D stacked architectures. In Proceedings of the Conference on Design, Automation and Test in Europe," *European Design and Automation Association,* pp. 111-116, 2010.

[18] H. Xu, Y. Wang and X. Han, "Analytical considerations of thermal storage and interface evolution of a PCM with/without porous media," *International Journal of Numerical Methods for Heat & Fluid Flow,* 2019.

[19] H. J. Xu, "Thermal transport in microchannels partially filled with micro-porous media involving flow inertia, flow/thermal slips, thermal non-equilibrium and thermal asymmetry," *International Communications in Heat and Mass Transfer,* vol. 110, p. 104404, 2020.

[20] J. H. Nazzi Ehms, R. De Césaro Oliveski, L. A. Oliveira Rocha, C. Biserni and M. Garai, "Fixed Grid Numerical Models for Solidification and Melting of Phase Change Materials (PCMs)," *Applied Sciences,* vol. 9, no. 20, p. 4334, 2019.

[21] J. N. Ehms, R. D. C. Oliveski, L. O. Rocha and C. Biserni, "Theoretical and numerical analysis on phase change materials (PCM): A case study of the solidification process of erythritol in spheres," *International Journal of Heat and Mass Transfer,* vol. 119, pp. 523-532, 2018.

[22] Y. T. Yang and Y. H. Wang, "Numerical simulation of three-dimensional transient cooling application on a portable electronic device using phase change material," *International Journal of thermal sciences,* vol. 51, pp. 155-162, 2012.

[23] Y. H. Wang and Y. T. Yang, "Three-dimensional transient cooling simulations of a portable electronic device using PCM (phase change materials) in multi-fin heat sink," *Energy,* vol. 36, no. 8, pp. 5214-5224, 2011.

[24] V. Shatikian, G. Ziskind and R. Letan, "Numerical investigation of a PCM-based heat sink with internal fins: constant heat flux," *International Journal of Heat and Mass Transfer,* vol. 51, no. 5-6, pp. 1488-1493, 2008.

[25] I. Assi, I. Mjallal, H. Farhat, M. Hammoud, S. Ali, A. Al Shaer and A. & Assi, "Using phase change material in heat sinks to cool electronics devices with intermittent usage," *IEEE 7th International Conference on Power and Energy Systems (ICPES),* pp. 66-69, 2017.

[26] G. Susman, Z. Dehouche, T. Cheechern and S. Craig, "Tests of prototype PCM 'sails' for office cooling," *Applied Thermal Engineering,* vol. 31, no. 5, pp. 717-726, 2011.

[27] K. C. Nayak, S. K. Saha, K. Srinivasan and P. Dutta, "A numerical model for heat sinks with phase change materials and thermal conductivity enhancers," *International Journal of Heat and Mass Transfer,* vol. 49, no. 11-12, pp. 1833-1844, 2006.

[28] J. A. Dantzig, "Modelling liquid–solid phase changes with melt convection," *International Journal for Numerical Methods in Engineering,* vol. 28, no. 8, pp. 1769-1785, 1989.

[29] A. Hasan, H. Hejase, S. Abdelbaqi, A. Assi and M. Hamdan, "Comparative Effectiveness of Different Phase Change Materials to Improve Cooling Performance of Heat Sinks for Electronic Devices," *Applied Sciences,* vol. 6, no. 9, p. 226, 2016.

[30] K. Kaygusuz, " Experimental and theoretical investigation of latent heat storage for water based solar heating systems," *Energy conversion and management,* vol. 36, no. 5, pp. 315-323, 1995.

[31] L. F. Cabeza, J. Illa, J. Roca, F. Badia, H. Mehling, S. Hiebler and F. Ziegler, "Middle term immersion corrosion tests on metal-salt hydrate pairs used for latent heat storage in the 32 to 36° C temperature range," *Materials and corrosion,* vol. 52, no. 10, pp. 748-754, 2001.

[32] F. Berroug, E. K. Lakhal, M. El Omari, M. Faraji and H. El Qarnia, "Thermal performance of a greenhouse with a phase change material north wall," *Energy and Buildings,* vol. 43, no. 11, pp. 3027-3035, 2011.

[33] V. V. Tyagi and D. Buddhi, "Thermal cycle testing of calcium chloride hexahydrate as a possible PCM for latent heat storage," *Solar Energy Materials and Solar Cells,* vol. 92, no. 8, pp. 891-899, 2008.